# Electron Interactions with $CHF_3$

**L. G. Christophorou,[a] J. K. Olthoff, and M. V. V. S. Rao**
*National Institute of Standards and Technology, Gaithersburg, Maryland 20899-0001*

Received August 6, 1996; revised manuscript received October 11, 1996

In this paper we assess and synthesize the available information on the cross sections and the rate coefficients for collisional interactions of trifluoromethane ($CHF_3$) with electrons in an effort to build a database on electronic and ionic collision processes that will aid the understanding of the behavior of $CHF_3$ in its use in manufacturing semiconductor devices and other applications. The limited data on the total and partial electron impact ionization cross sections, total and partial cross sections for electron impact dissociation of $CHF_3$ into neutral species, electron-impact induced line and continuous light emission from $CHF_3$, negative ion states of $CHF_3$, and the energetics of ionization, dissociation, and attachment are summarized and discussed. Besides some recent unpublished measurements of the total electron scattering cross section below 20 eV, to our knowledge no measurements are available of the cross sections of any of the electron scattering processes (elastic, momentum, vibrational, inelastic, etc.) or the electron transport, attachment, and ionization coefficients. While the available information is meager, the synthesis of the existing knowledge and the background information provided in the paper can be helpful for modeling plasma reactors. Clearly, more measurements and calculations are needed of the cross sections for virtually all fundamental electron impact processes for this plasma processing gas. Measurements of the transport, attachment, and ionization coefficients over wide ranges of the density reduced electric field are also needed.  [S0047-2689(97)00201-8]

Key words: attachment; $CHF_3$; cross sections; dissociation; electron scattering; emission; fluoroform; ionization; transport; trifluoromethane.

## Contents



### List of Tables



[a]Also at Department of Physics, The University of Tennessee, Knoxville, TN 37996-1200.

### List of Figures



## 1. Introduction

Trifluoromethane or fluoroform ($CHF_3$) is a plasma processing gas. As a fluorohydrocarbon, it does not contain atomic chlorine and is, thus, not destructive of stratospheric ozone. Trifluoromethane is, however, a greenhouse gas. It has a global warming potential over a 100-year time horizon of 12 100 relative to the global warming potential of $CO_2$ over the same time period.[1] The global warming potential of $CHF_3$ is about twice as large as that of $CF_4$, which is also used in plasma processing. However, the lifetime of $CHF_3$ in the atmosphere is much shorter[1] (250 years) compared to the lifetime of $CF_4$ (50 000 years).[1] This makes $CHF_3$ a desirable substitute for $CF_4$ in some industrial applications.

In this paper, as in a previous study[2] for $CF_4$, we assess and synthesize the available information on the cross sections and the rate coefficients for collisional interactions of $CHF_3$ with electrons. Definitions of the symbols we use to describe the various collision processes discussed in this paper are given in Table 1. This study is part of an effort to build a database on electronic and ionic collision processes that will aid the understanding of the behavior of $CHF_3$ in its use in manufacturing semiconductor devices and other appli-

TABLE 1. Definition of symbols

| Symbol | Definition | Common scale and units |
|---|---|---|
| $\sigma_{sc,t}(\varepsilon)$ | Total electron scattering cross section | $10^{-20}$ m$^2$ |
| $\sigma_{i,t}(\varepsilon)$ | Total electron impact ionization cross section | $10^{-20}$ m$^2$ |
| $\sigma_{i,part}(\varepsilon)$ | Partial dissociative ionization cross section | $10^{-20}$ m$^2$ |
| $\sigma_{diss,t}(\varepsilon)$ | Total electron impact dissociation cross section | $10^{-20}$ m$^2$ |
| $\sigma_{diss,n,part}(\varepsilon)$ | Partial cross section for electron impact dissociation into neutral fragments | $10^{-20}$ m$^2$ |
| $\sigma_{diss,n,t}(\varepsilon)$ | Total electron impact dissociation into neutral species | $10^{-20}$ m$^2$ |
| $\sigma_{em}$ | Emission cross section | $10^{-19}$ cm$^2$ |
| $(k_a)_{th}$ | Thermal electron attachment rate constant | $10^{-14}$ cm$^3$ s$^{-1}$ |

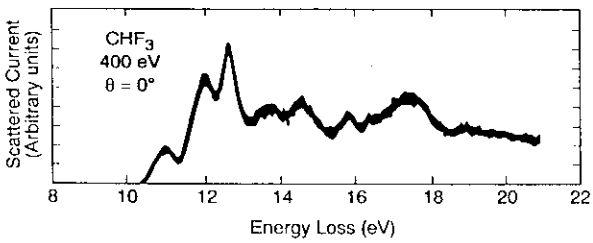


FIG. 1. Electron impact energy loss spectrum of $CHF_3$ obtained (Ref. 13) with 400 eV incident electrons scattered at an angle $\theta$=0°.

cations. Unlike our earlier work on $CF_4$, however, the data on this molecule are insufficient to allow a recommendation of specific data at this time.

## 2. Electronic and Molecular Structure

The structure of the $CHF_3$ molecule is a symmetric top of the $C_{3v}$ point group. The outer electronic orbital structure[3–6] of $CHF_3$ is

$$\ldots(4a_1)^2(5a_1)^2(3e)^4(4e)^4(5e)^4(1a_2)^2(6a_1)^2.$$

In contrast to $CF_4$ which is nonpolar, the $CHF_3$ molecule is polar. Its electric dipole moment has been reported to be $5.504\times10^{-30}$ C m (=1.65 D).[7–9] As a consequence of its dipole moment, $CHF_3$ has a strong rotational spectrum (see, e.g., Cazzoli *et al.*[10]). The $CHF_3$ molecule also has a sizeable static polarizability. Beran and Kevan[11] calculated the static polarizability of $CHF_3$ using three different methods. Their values are: $26.9\times10^{-25}$ cm$^3$, $27.8\times10^{-25}$ cm$^3$, and $35.5\times10^{-25}$ cm$^3$. Sutter and Cole[9] obtained the value $35.7\times10^{-25}$ cm$^3$ from dielectric constant measurements (see Kobayashi *et al.*[12] for frequency-dependent polarizabilities of $CHF_3$).

There have been a number of electron-impact energy loss, photoelectron, and photoabsorption studies of $CHF_3$ and we only refer to representatives of such data below. Figure 1 shows the electron-impact energy loss spectrum[13] of $CHF_3$ up to 21 eV. The spectrum was obtained using electrons with 400 eV incident energy scattered at an angle $\theta = 0°$. Table 2 lists the measured vertical excitation and ionization energies of $CHF_3$ with assignments as given by Harshbarger *et al.*[13] Table 2 also lists similar data[6] derived from measurements of the generalized oscillator strengths of valence electronic transitions of $CHF_3$ as a function of energy loss (0 eV to 15 eV) using angle-resolved electron energy loss-spectroscopy at 2.5 keV incident electrons. A more recent *ab initio* configuration interaction calculation[14] confirmed the Rydberg nature of the electronic transitions that constitute the absorption spectrum of $CHF_3$, but maintained that "most of the transitions correspond to relatively unlocalized charge transfers and that the distinction between types $s$, $p$, or $d$ Rydberg states is difficult to establish."

The vacuum ultraviolet absorption spectrum of $CHF_3$ has been reported by Sauvageau *et al.*[15] between 60 nm and 120 nm and by Wu *et al.*[4] in the wavelength range of 18 nm to 72 nm using synchrotron radiation. As an example of this type of measurement we reproduce in Fig. 2 and list in Table 3 the data of Wu *et al.*[4] Adiabatic and vertical ionization energies[3,16–18] of $CHF_3$ determined from photoelectron spectra are given in Table 4 (see also a relevant review by Bieri *et al.*[19]). Interestingly, in optical studies, vibrational fine structure has been observed for some excited electronic states,[4,15,16] showing that "stable" excited electronic states exist for this molecule.

The energies of the six fundamental vibrational modes[20,21] of $CHF_3$ $\nu_1$, $\nu_2$, $\nu_3$, $\nu_4$, $\nu_5$, and $\nu_6$ are (0.3763, 0.1415, 0.0864, 0.1708, 0.1435, and 0.063) eV, respectively.

TABLE 2. Vertical excitation and ionization energies of $CHF_3$ with assignments (from Harshbarger *et al.*—Ref. 13 unless otherwise noted)

| Excitation energy (eV) | Ionization energy (eV) | Assignment |
|---|---|---|
| 10.92; 11.1[a] | | $6a_1\rightarrow3s$ |
| 11.95; 11.9[a] | | $6a_1\rightarrow3p$ |
| 12.58; 12.7[a] | | $5e\rightarrow3s$ |
| 13.65; 13.7[a] | | $5e\rightarrow3p$ |
| | | $4e\rightarrow3s$ |
| 14.49 | | $4e\rightarrow3p$ |
| | 14.8 | $6a_1$ |
| | 15.5 | $1a_2$ |
| 15.76 | | $4e\rightarrow3d$ |
| | 16.2 | $5e$ |
| 16.42 | | $3e\rightarrow3s$ |
| | | $5a_1\rightarrow3s$ |
| | 17.24 | $4e$ |
| 17.4 | | $3e\rightarrow3p$ |
| | | $5a_1\rightarrow3p$ |
| 19.14 | | $3e\rightarrow3d$ |
| | | $5a_1\rightarrow3d$ |
| | 20.84 | $3e$ |
| | | $5a_1$ |

[a]Reference 6.

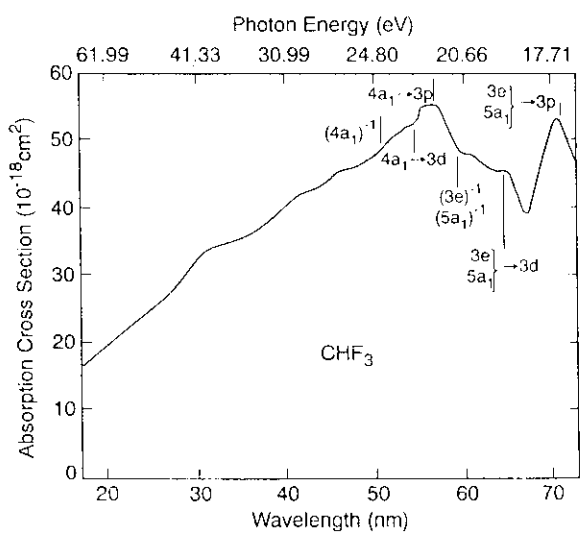


FIG. 2. Absorption cross section of $CHF_3$ in the wavelength range 17.5 nm to 76 nm. Indicated in the figure are the positions of the probable Rydberg states and their ion states (from Wu *et al.*—Ref. 4).

TABLE 3. Absorption cross section of $CHF_3$ (from Wu *et al.*—Ref. 4)

| Wavelength (nm) | Cross section ($10^{-18}$ cm$^2$) |
|---|---|
| 18 | 17.5 |
| 20 | 19.6 |
| 22 | 21.8 |
| 24 | 23.9 |
| 26 | 26.3 |
| 28 | 29.0 |
| 30 | 32.5 |
| 32 | 34.6 |
| 34 | 35.1 |
| 36 | 36.3 |
| 38 | 38.4 |
| 40 | 40.4 |
| 42 | 42.8 |
| 44 | 44.0 |
| 46 | 45.7 |
| 48 | 46.6 |
| 50 | 48.0 |
| 52 | 50.2 |
| 54 | 52.1 |
| 56 | 55.3 |
| 58 | 52.0 |
| 60 | 48.3 |
| 62 | 46.7 |
| 64 | 45.6 |
| 66 | 42.8 |
| 68 | 41.7 |
| 70 | 53.1 |
| 72 | 49.3 |

## 3. Electron Scattering

The sizeable electric dipole moment of the $CHF_3$ molecule allows for a determination of an estimate for the momentum transfer and total electron scattering cross sections at low electron energies (thermal and near thermal). First, the Born approximation theory of Altshuler[22] predicts that the momentum transfer cross section $\sigma_m(\nu)$ varies with the incident electron velocity $\nu$ as

$$\sigma_m(\nu) = 1.72D^2/\nu^2, \tag{1}$$

TABLE 4. Adiabatic and vertical ionization energies of $CHF_3$ determined from photoelectron spectra (from Ref. 3 unless otherwise indicated)

| Orbital | Adiabatic ionization energy (eV) | Vertical ionization energy (eV) |
|---|---|---|
| $6a_1$ | ≥13.8; 13.84;[b] 14.19;[c] 13.86[d] | 14.8; 14.77[d] |
| $1a_2$ | | 15.5; 15.46[d] |
| $5e$ | | 16.2; 16.16[d] |
| $4e$ | 17.11; 17.13[d] | 17.24; 17.26[d] |
| $3e$ | | |
| | 20.6[a]; 20.05[d] | 19.84[a]; ~21[d] |
| $5a_1$ | | |
| $4a_1$ | ≥24.34 | 24.44 |

[a]Unresolved blend of two or more transitions.
[b]Reference 16.
[c]Reference 17.
[d]Reference 18.

where the dipole moment, $D$, is in debye units (1 D=3.3356×10$^{-30}$ C m) and the electron velocity, $\nu$, is in cm s$^{-1}$. Christophorou and Christodoulides[23] have found that for the molecules they studied with electric dipole moments in the range $2\times10^{-30}$ C m $< D < 13.68\times10^{-30}$ C m, the experimental cross sections for electrons having a Maxwellian energy distribution are within 50% of those calculated via Eq. (1). We employed Eq. (1) and obtained the momentum transfer cross section shown in Fig. 3 by the broken line using $5.504\times10^{-30}$ C m (=1.65 D)[7–9] for the $D$ of $CHF_3$. Second, Christophorou and Christodoulides[23,24] approximated the total electron scattering cross section for thermal and near thermal electron scattering for strongly polar molecules as

$$\sigma_{sc,t}(\nu) \approx A_1/\nu^2, \tag{2}$$

where $A_1$ is a constant equal to $7.7574\times10^5$ $S^{-1}$ and $S = w/(E/P)$. The slope, $S$, is determined in the low $E/P$ region where the electron drift velocity, $w$, varies linearly with $E/P$ ($E$ is the applied uniform electric field and $P$ is the total gas pressure at the temperature of the experiment). We have used the value $1.773\times10^7$ cm$^2$ Pa V$^{-1}$ s$^{-1}$ (=$13.3\times10^4$ cm$^2$ Torr V$^{-1}$ s$^{-1}$) of $S$ reported by Christophorou *et al.*[25] for $E/N < 3.69\times10^{-17}$ V cm$^2$ ($E/P < 1.2$ V cm$^{-1}$ Torr$^{-1}$) and estimated the electron scattering cross section, $\sigma_{sc,t}(\nu)$, at low energies shown in Fig. 3 by the open triangle line. The total cross section we determined via Eq. (2) is ~25% higher than the momentum transfer cross section determined via Eq. (1). The cross sections determined through (1) and (2) are very large at low electron energies.

In Fig. 3 are also plotted (open circle line) recent unpublished measurements of $\sigma_{sc,t}(\varepsilon)$ by Sanabia and Moore[26] between about 0.1 eV and 20 eV. These data clearly fall below the calculated values for energies less than about 0.7 eV. In this low energy region the calculated cross sections can be useful as an estimate in the absence of accurate direct measurements. They are, however, approximate and are expected to fall below the true total electron scattering cross section values progressively by larger amounts as the energy is increased above about 1 eV, as is indeed the case (Fig. 3). For example, in the case of $H_2O$ ($D=6.17\times10^{-30}$ C m) and $NH_3$ ($D=4.87\times10^{-30}$ C m) the total electron scattering cross sections determined via (2) are compatible with the experimental measurements below about 2 eV, but begin to fall below the experimental values progressively by larger amounts as the electron energy is increased above ~2 eV (see Fig. 3 of Ref. 25 and Fig. 4 of Ref. 27). We have determined a suggested set of values for $\sigma_{sc,t}(\varepsilon)$ by accepting the calculated values of $\sigma_{sc,t}(\varepsilon)$ below ~0.7 eV and merging these with the measured values of Sanabia and Moore[26] above this energy. These cross sections are shown in Fig. 3 by the solid line and are listed in Table 5 as the suggested set of values for $\sigma_{sc,t}(\varepsilon)$ of $CHF_3$ in the absence of more reliable data.

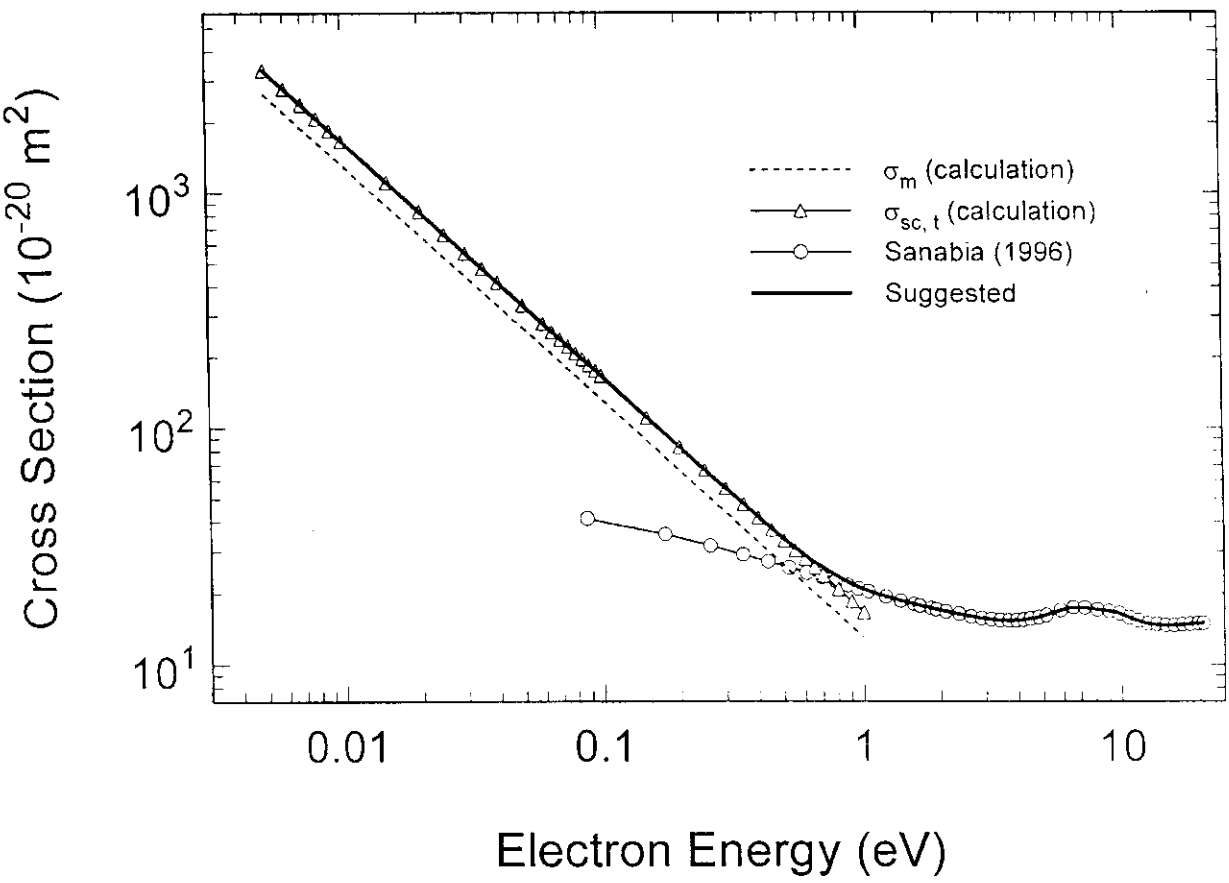


FIG. 3. Calculated momentum transfer (- - -) and total (△) electron scattering cross sections for $CHF_3$ at low electron energies. Measured—Ref. 26 (○) and suggested (—) total electron scattering cross sections (see the text).

## 4. Electron Impact Ionization

There have been few measurements of the partial and total electron impact ionization cross sections of $CHF_3$. Poll and Meichsner[28] measured the partial ionization cross sections for the following ions: $CF_3^+$, $CHF_2^+ + CF_2^+$, and $CF^+$, and their results (obtained from Fig. 2(j) of their paper) are listed in Table 6 and are plotted in Fig. 4. We determined the sum $\sigma_{i,\,part,\,t}(\varepsilon)$ of these partial cross sections which is listed in column 5 of Table 6. A second set of measurements of the partial ionization cross sections was made by Goto *et al.*[29] for the following ions: $CF_3^+$, $CHF_2^+$, $CF_2^+$, $CHF^+$, $CF^+$, $CH^+$, and $F^+$, and these are listed in Table 7 and are plotted in Fig. 5. Their sum $\sigma_{i,\,part,\,t}(\varepsilon)$ is given in column 9 of Table 7.

Figure 6 compares the partial ionization cross sections, $\sigma_{i,\,part}(\varepsilon)$, of Poll and Meichsner[28] on $CF_3^+$, $CHF_2^+ + CF_2^+$, and $CF^+$ with the respective data of Goto *et al.*[29] There are substantial differences in the two sets of data which depend on the particular ion; the largest difference is for the sum of the two ions $CHF_2^+ + CF_2^+$.

A comparison of the sum $\sigma_{i,\,part,\,t}(\varepsilon)$ of the partial ionization cross sections, which should approximate $\sigma_{i,\,t}(\varepsilon)$, of Poll and Meichsner[28] and of Goto *et al.*[29] is made in Fig. 7. Clearly the two sets of data differ and since we have insufficient basis to judge their respective validity, we have averaged the two sets of values and have taken this average to be a "recommended" set for the total ionization cross section, $\sigma_{i,\,t}(\varepsilon)$. The $\sigma_{i,\,part,\,t}(\varepsilon)$ of the two experimental groups and their average are listed in Table 8. Table 8 also gives the early measurement of the total ionization cross section of $CHF_3$ made by Beran and Kevan[30] at three values of the incident electron energy. The three sets of values are compared in Fig. 7 with the recent unpublished results of a calculation of the total ionization cross section, $\sigma_{i,\,t}(\varepsilon)$, of $CHF_3$ by Kim.[31] The result of Kim's calculation is in reasonable agreement with the measurements below about 50 eV, but the calculated cross section is much lower than the experimental values at higher energies. Kim used a model[32] which combines binary encounter theory and the Bethe theory of electron impact ionization.

Since all electronically excited states of the $CHF_3$ molecule dissociate or predissociate[33] (no parent $CHF_3^+$ has been observed although some optical emission resulting from electron impact on $CHF_3$ has been attributed to $CHF_3^+$, see Sec. 8), and since the electron impact dissociation cross sections of $CHF_3$ into neutral species are small (see Sec. 5), the total dissociation cross section should be about equal to the total dissociative ionization cross section at energies sufficiently above the ionization threshold.

TABLE 5. Total electron scattering cross section, $\sigma_{sc,t}(\varepsilon)$, of $CHF_3$ in units of $10^{-20}$ m$^2$ (see the text)

| Electron energy (eV) | $\sigma_{sc,t}(\varepsilon)$ ($10^{-20}$ m$^2$) |
|---|---|
| 0.005 | 3321.2 |
| 0.006 | 2768.9 |
| 0.007 | 2373.4 |
| 0.008 | 2075.3 |
| 0.009 | 1845.2 |
| 0.01 | 1660.4 |
| 0.015 | 1107.2 |
| 0.02 | 830.4 |
| 0.025 | 664.3 |
| 0.03 | 553.5 |
| 0.035 | 474.4 |
| 0.04 | 415.2 |
| 0.045 | 369.0 |
| 0.05 | 332.1 |
| 0.06 | 276.8 |
| 0.07 | 237.2 |
| 0.08 | 207.6 |
| 0.09 | 184.5 |
| 0.10 | 166.1 |
| 0.15 | 110.7 |
| 0.20 | 83.0 |
| 0.25 | 66.4 |
| 0.30 | 55.3 |
| 0.35 | 47.6 |
| 0.40 | 41.7 |
| 0.45 | 37.3 |
| 0.50 | 33.7 |
| 0.60 | 28.8 |
| 0.70 | 25.5 |
| 0.80 | 23.4 |
| 0.90 | 21.8 |
| 1.0 | 20.8 |
| 1.5 | 18.2 |
| 2.0 | 16.9 |
| 2.5 | 16.1 |
| 3.0 | 15.6 |
| 3.5 | 15.4 |
| 4.0 | 15.4 |
| 4.5 | 15.7 |
| 5.0 | 16.1 |
| 6.0 | 17.0 |
| 7.0 | 17.3 |
| 8.0 | 17.1 |
| 9.0 | 16.7 |
| 10 | 16.3 |
| 12 | 15.1 |
| 14 | 14.7 |
| 16 | 14.7 |
| 18 | 14.8 |
| 20 | 14.9 |

Table 9 lists the energy thresholds of a number of reactions leading to positive ions by electron impact on $CHF_3$ (Refs. 29 and 34–36). The larger positive ions have lower energy thresholds. By selectively choosing the electron energy, one may eliminate the production of ions with higher energy onsets using the information in this table.

TABLE 6. Partial dissociative ionization cross sections, $\sigma_{i,\,part}(\varepsilon)$, of $CHF_3$ in units of $10^{-20}$ m$^2$ (from Ref. 28); $\sigma_{i,\,part,\,t}(\varepsilon)$ is the sum of the cross sections in columns 2–4

| Energy (eV) | $\sigma_{i,\,part}(\varepsilon)$ $CF_3^+$ | $\sigma_{i,\,part}(\varepsilon)$ $CHF_2^+ + CF_2^+$ | $\sigma_{i,\,part}(\varepsilon)$ $CF^+$ | $\sigma_{i,\,part,\,t}(\varepsilon)$ |
|---|---|---|---|---|
| 20 | 0.18 | 0.23 | 0.001 | 0.41 |
| 25 | 0.36 | 0.90 | 0.25 | 1.51 |
| 30 | 0.53 | 1.54 | 0.71 | 2.78 |
| 35 | 0.69 | 2.13 | 1.07 | 3.89 |
| 40 | 0.82 | 2.64 | 1.40 | 4.86 |
| 45 | 0.94 | 3.04 | 1.67 | 5.65 |
| 50 | 1.03 | 3.36 | 1.91 | 6.30 |
| 60 | 1.18 | 3.77 | 2.24 | 7.19 |
| 70 | 1.28 | 3.93 | 2.52 | 7.73 |
| 80 | 1.35 | 4.00 | 2.69 | 8.04 |
| 90 | 1.40 | 4.03 | 2.82 | 8.25 |
| 100 | 1.44 | 4.02 | 2.90 | 8.36 |
| 110 | 1.47 | 4.00 | 2.96 | 8.43 |
| 120 | 1.48 | 3.95 | 3.00 | 8.43 |

## 5. Electron Impact Dissociation Producing Neutral Species

As in the case of $CF_4$, the $CHF_3$ molecules predominantly dissociate or predissociate upon electronic excitation. Although the observation of vibrational structure for some electronic transitions would indicate stable excited electronic states, dissociation is the dominant process that follows elec-

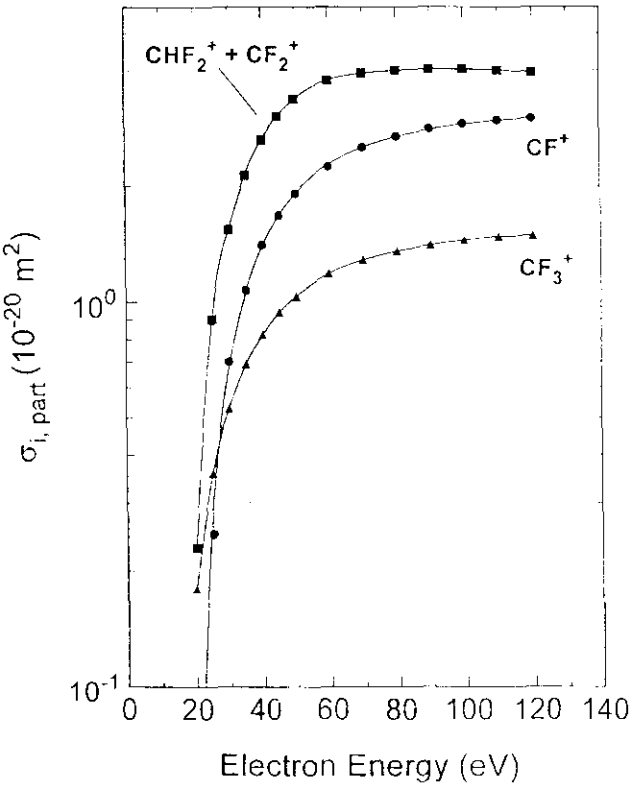


FIG. 4. Partial electron impact ionization cross sections, $\sigma_{i,\,part}(\varepsilon)$, of $CHF_3$ for the production of $CF_3^+$, $CHF_2^+ + CF_2^+$, and $CF^+$ (data of Poll and Meichsner—Ref. 28).

TABLE 7. Partial dissociative ionization cross sections, $\sigma_{i,\,part}(\varepsilon)$, of $CHF_3$ in units of $10^{-20}\,m^2$ (from Ref. 29)

| Energy (eV) | $\sigma_{i,\,part}(\varepsilon)$ $CF_3^+$ | $\sigma_{i,\,part}(\varepsilon)$ $CHF_2^+$ | $\sigma_{i,\,part}(\varepsilon)$ $CF_2^+$ | $\sigma_{i,\,part}(\varepsilon)$ $CHF^+$ | $\sigma_{i,\,part}(\varepsilon)$ $CF^+$ | $\sigma_{i,\,part}(\varepsilon)$ $CH^+$ | $\sigma_{i,\,part}(\varepsilon)$ $F^+$ | $\sigma_{i,\,part,\,t}(\varepsilon)$[a] |
|---|---|---|---|---|---|---|---|---|
| 20 | 0.12 | 0.01 | | | | | | 0.13 |
| 25 | 0.38 | 0.06 | 0.01 | 0.03 | 0.06 | | | 0.54 |
| 30 | 0.64 | 0.12 | 0.02 | 0.05 | 0.26 | | | 1.09 |
| 35 | 1.02 | 0.19 | 0.03 | 0.10 | 0.53 | | | 1.87 |
| 40 | 1.30 | 0.25 | 0.05 | 0.15 | 0.81 | 0.01 | 0.01 | 2.58 |
| 45 | 1.52 | 0.30 | 0.07 | 0.20 | 1.12 | 0.01 | 0.02 | 3.24 |
| 50 | 1.70 | 0.34 | 0.09 | 0.26 | 1.46 | 0.02 | 0.04 | 3.91 |
| 60 | 1.88 | 0.39 | 0.13 | 0.36 | 1.94 | 0.02 | 0.07 | 4.79 |
| 70 | 2.04 | 0.41 | 0.17 | 0.42 | 2.35 | 0.02 | 0.10 | 5.52 |
| 80 | 2.15 | 0.42 | 0.19 | 0.49 | 2.50 | 0.03 | 0.12 | 5.90 |
| 90 | 2.12 | 0.43 | 0.21 | 0.53 | 2.71 | 0.03 | 0.13 | 6.16 |
| 100 | 2.16 | 0.43 | 0.23 | 0.56 | 2.75 | 0.02 | 0.14 | 6.29 |
| 110 | 2.18 | 0.44 | 0.24 | 0.58 | 2.87 | 0.02 | 0.15 | 6.48 |
| 120 | 2.22 | 0.44 | 0.25 | 0.60 | 2.88 | 0.02 | 0.15 | 6.56 |

[a]The sum of columns 2–8.

tronic excitation. Thus, Winters and Inokuti[33] argued that the total dissociation cross section of $CHF_3$ is equal to the total cross section for electronic excitation (the sum of the cross sections for excitation to all electronic and ionic states). The data of Winters and Inokuti on the total dissociation cross section of $CHF_3$ up to 300 eV, are listed in Table 10 and are plotted in Fig. 8.

There has been a study by Goto *et al.*[29] reporting partial cross sections, $\sigma_{diss,\,n,\,part}(\varepsilon)$, for dissociation of $CHF_3$ by electron impact into the neutral fragments $CF_3$, $CHF_2$, $CF_2$, CHF, and CF. The reported cross sections are listed in Table 11 and are plotted in Fig. 9. Column 7 of Table 11 gives the sum, $\sigma_{diss,\,n,\,t}(\varepsilon)$, of the partial dissociation cross sections in columns 2–6.

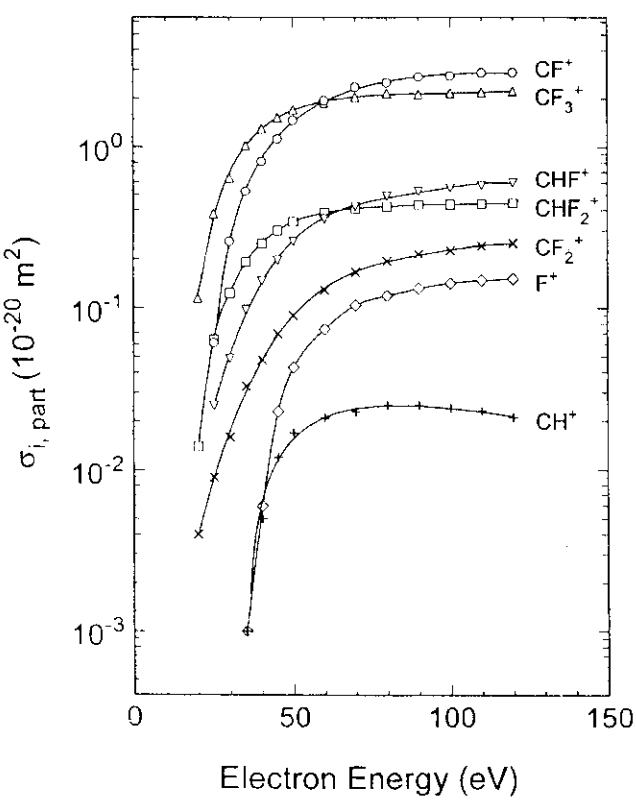


FIG. 5. Partial electron impact ionization cross sections, $\sigma_{i,\,part}(\varepsilon)$, of $CHF_3$ for the production of $CF_3^+$, $CHF_2^+$, $CF_2^+$, $CHF^+$, $CF^+$, $CH^+$, and $F^+$ (data of Goto *et al.*—Ref. 29).

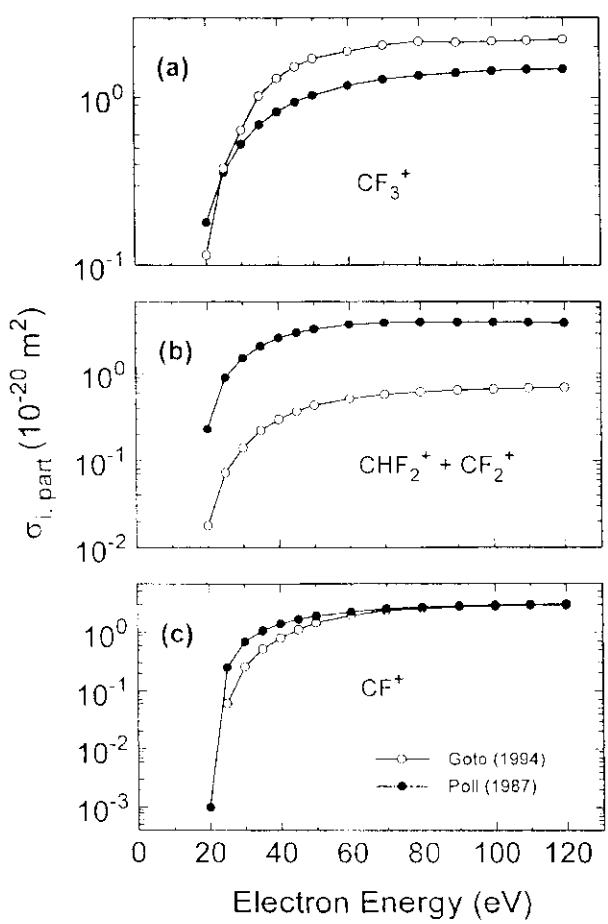


FIG. 6. Comparison of the measurements of Poll and Meichsner (Ref. 28) of the $\sigma_{i,\,part}(\varepsilon)$ for $CF_3^+$, $CHF_2^+ + CF_2^+$, and $CF^+$ with the measurements of Goto *et al.*—Ref. 29 for the same ions. Since Poll and Meichsner reported a cross section for the sum of $CHF_2^+$ and $CF_2^+$ the corresponding cross sections for the two ions reported by Goto *et al.* were summed up and plotted in (b).

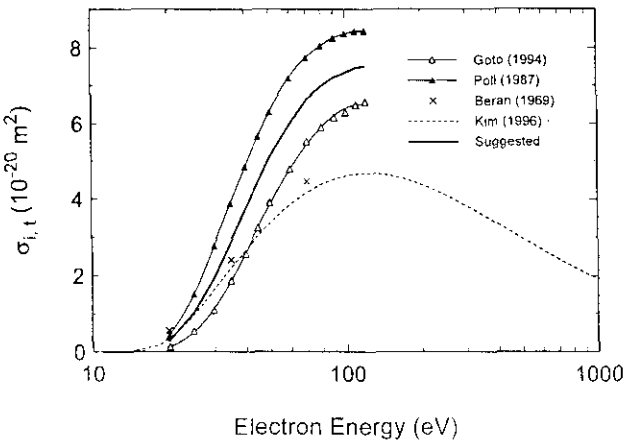


FIG. 7. Total electron impact ionization cross section, $\sigma_{i,t}(\varepsilon)$, for $CHF_3$ (see the text). Experimental values: ×, Ref. 30; ▲, Ref. 28 (Column 5 of Table 6); △, Ref. 29 (Column 9 of Table 7); —, average of data from Refs. 28 and 29 (Column 5 of Table 8). Calculated values; ---, Ref. 31.

The cross sections of Goto *et al.*[29] have subsequently been revised by Sugai *et al.*[37] using the absolute cross sections for electron impact dissociation of the $CF_x(x = 1-3)$ radicals reported by Tarnovsky *et al.*[38,39] The revised data of Sugai *et al.*[37] for the $CF_3$, $CF_2$, and CF radicals are given in Table 12 and are plotted in Fig. 10. Column 5 of Table 12 lists the sum, $\sigma_{\text{diss, n, t}}(\varepsilon)$, of the partial cross sections for the three neutral fragments. The revised cross sections are very small and differ from the original data (Table 11) by factors of up to 16 (see Fig. 11). The most abundant neutral fragments are the $CF_3$ and CF radicals.

The sum of the partial dissociation cross sections into neutrals, $\sigma_{\text{diss, n, t}}(\varepsilon)$, are listed in the last columns of Tables 11 and 12 and are plotted in Fig. 12. They represent an estimate of the total cross section for electron impact dissociation of the $CHF_3$ molecule into neutral fragments. Even though the cross sections $\sigma_{\text{diss, n, t}}(\varepsilon)$ in Table 12 do not include the con-

TABLE 8. Total electron impact ionization cross section, $\sigma_{i,t}(\varepsilon)$, for $CHF_3$ in units of $10^{-20}$ m$^2$

| Energy (eV) | Ref. 30 | Ref. 28[a] | Ref. 29[b] | $\sigma_{i,t}(\varepsilon)$[c] |
|---|---|---|---|---|
| 20 | 0.55 | 0.41 | 0.13 | 0.27 |
| 25 | | 1.51 | 0.54 | 1.03 |
| 30 | | 2.78 | 1.09 | 1.94 |
| 35 | 2.41 | 3.89 | 1.87 | 2.88 |
| 40 | | 4.86 | 2.57 | 3.72 |
| 45 | | 5.65 | 3.24 | 4.45 |
| 50 | | 6.30 | 3.91 | 5.11 |
| 60 | | 7.19 | 4.79 | 5.99 |
| 70 | 4.47 | 7.73 | 5.52 | 6.63 |
| 80 | | 8.04 | 5.90 | 6.97 |
| 90 | | 8.25 | 6.16 | 7.21 |
| 100 | | 8.36 | 6.29 | 7.33 |
| 110 | | 8.43 | 6.48 | 7.46 |
| 120 | | 8.43 | 6.56 | 7.50 |

[a] $\sigma_{i,\text{part},t}(\varepsilon)$; last column of Table 6.
[b] $\sigma_{i,\text{part},t}(\varepsilon)$; last column of Table 7.
[c] $\sigma_{i,t}(\varepsilon)$: average of columns 3 and 4.

TABLE 9. Threshold energies for "appearance" of positive ions by electron impact on $CHF_3$

| Reaction | Threshold energy (eV) | Reference |
|---|---|---|
| $CHF_3 + e \rightarrow CF_3^+ + H$ | 15.2 | 29 |
| | 14.67 | 34 |
| | 14.53 | 35 |
| | 14.42 | 36 |
| $CHF_3 + e \rightarrow CHF_2^+ + F$ | 16.8 | 29 |
| | 16.4 | 34 |
| | 15.75 | 36 |
| $CHF_3 + e \rightarrow CF_2^+ + HF$ | 17.6 | 29 |
| $\rightarrow CF_2^+ + H + F$ | 17.5 | 34 |
| | 20.2 | 36 |
| $CHF_3 + e \rightarrow CHF^+ + F_2$ | 19.8 | 29 |
| $CHF_3 + e \rightarrow CF^+ + HF + F$ | 20.9 | 29 |
| | 20.75 | 36 |
| | 20.2 | 34 |
| $CHF_3 + e \rightarrow CH^+ + F_2 + F$ | 33.5 | 29 |
| $CHF_3 + e \rightarrow F^+ + \ldots$ | 37.0 | 29 |

TABLE 10. Total electron impact dissociation cross section, $\sigma_{\text{diss, t}}(\varepsilon)$, for $CHF_3$ in units of $10^{-20}$ m$^2$ (data of Ref. 33)

| Energy (eV) | $\sigma_{\text{diss, t}}(\varepsilon)$ |
|---|---|
| 22 | 2.4 |
| 72 | 5.5 |
| 100 | 5.8 |
| 125 | 5.7 |
| 200 | 5.4 |
| 300 | 4.9 |

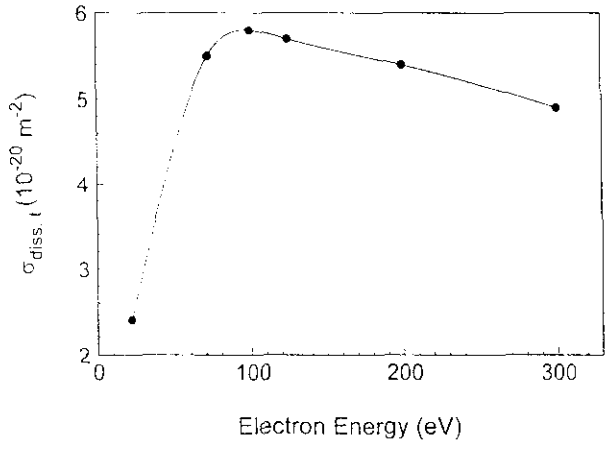


FIG. 8. Total electron impact dissociation cross section, $\sigma_{\text{diss, t}}(\varepsilon)$, (from Winters and Inokuti—Ref. 33).

TABLE 11. Cross sections, $\sigma_{diss,\,n,\,part}(\varepsilon)$, for electron impact dissociation of $CHF_3$ into neutral fragments in units of $10^{-20}\,m^2$ (from Ref. 29). The last column is the sum, $\sigma_{diss,\,n,\,t}(\varepsilon)$, of the respective cross sections in columns 2–6

| Energy (eV) | $\sigma_{diss,\,n,\,part}(\varepsilon)$ $CF_3$ | $\sigma_{diss,\,n,\,part}(\varepsilon)$ $CHF_2$ | $\sigma_{diss,\,n,\,part}(\varepsilon)$ $CF_2$ | $\sigma_{diss,\,n,\,part}(\varepsilon)$ CHF | $\sigma_{diss,\,n,\,part}(\varepsilon)$ CF | $\sigma_{diss,\,n,\,t}(\varepsilon)$ |
|---|---|---|---|---|---|---|
| 20 | 0.02 | 0.001 | | | 0.01 | 0.031 |
| 25 | 0.03 | 0.002 | | | 0.16 | 0.192 |
| 30 | 0.05 | 0.003 | 0.014 | | 0.22 | 0.287 |
| 35 | 0.08 | 0.004 | 0.025 | | 0.23 | 0.339 |
| 40 | 0.10 | 0.005 | 0.040 | | 0.24 | 0.385 |
| 50 | 0.24 | 0.008 | 0.075 | 0.002 | 0.23 | 0.555 |
| 60 | 0.33 | 0.010 | 0.098 | 0.002 | 0.22 | 0.660 |
| 70 | 0.37 | 0.017 | 0.104 | 0.004 | 0.21 | 0.705 |
| 80 | 0.38 | 0.024 | 0.099 | 0.004 | 0.19 | 0.697 |
| 90 | 0.46 | 0.027 | 0.092 | 0.005 | 0.20 | 0.784 |
| 100 | 0.49 | 0.032 | 0.092 | 0.006 | 0.18 | 0.800 |
| 110 | 0.50 | 0.034 | 0.094 | 0.008 | 0.21 | 0.846 |
| 120 | 0.48 | 0.038 | 0.090 | 0.011 | 0.18 | 0.799 |
| 130 | 0.47 | 0.039 | 0.086 | 0.014 | 0.18 | 0.789 |
| 140 | 0.45 | 0.040 | 0.088 | 0.015 | 0.19 | 0.783 |
| 150 | 0.44 | 0.038 | 0.080 | 0.016 | 0.16 | 0.734 |
| 160 | 0.45 | 0.037 | 0.075 | 0.019 | 0.18 | 0.761 |
| 170 | 0.43 | 0.038 | 0.074 | 0.019 | 0.19 | 0.751 |
| 180 | 0.44 | 0.038 | 0.076 | 0.019 | 0.20 | 0.773 |
| 190 | 0.45 | 0.041 | 0.073 | 0.018 | 0.16 | 0.742 |
| 200 | 0.44 | 0.040 | 0.076 | 0.019 | 0.20 | 0.775 |

tributions from the production of the neutral species $CHF_2$ and CHF, the contribution to the magnitude of $\sigma_{diss,\,n,\,t}(\varepsilon)$ from the cross sections for these two neutral species is small (see Table 11).

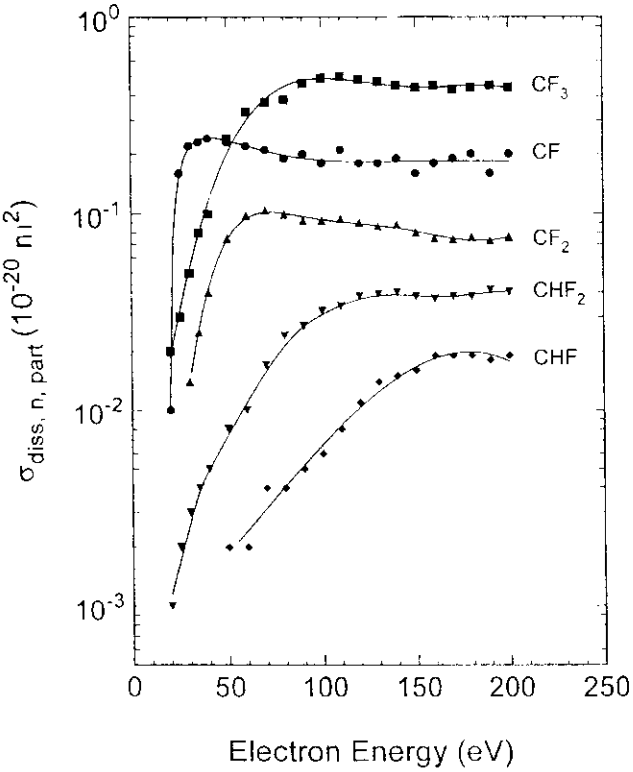


FIG. 9. Partial cross sections, $\sigma_{diss,\,n,\,part}(\varepsilon)$, for electron impact dissociation of $CHF_3$ into the neutral fragments $CF_3$, $CHF_2$, $CF_2$, CHF, and CF (data of Goto *et al.*—Ref. 29).

The data in Fig. 12 can be compared with the difference $\sigma_{diss,\,t}(\varepsilon)-\sigma_{i,\,t}(\varepsilon)\approx\sigma_{diss,\,n,\,t}(\varepsilon)$. We estimated this difference using the limited measurements of $\sigma_{diss,\,t}(\varepsilon)$ in Fig. 8 and the values of $\sigma_{i,\,t}(\varepsilon)$ shown in Fig. 7 by the solid line. While the uncertainty of the resultant total dissociation cross section into neutral fragments is very large, the values of

TABLE 12. Cross sections $\sigma_{diss,\,n,\,t}(\varepsilon)$ for electron impact dissociation of $CHF_3$ into the neutral fragments $CF_3$, $CF_2$, and CF in units of $10^{-20}\,m^2$ (data of Goto *et al.*—Ref. 29—as revised by Sugai *et al.*—Ref. 37). The last column is the sum, $\sigma_{diss,\,n,\,t}(\varepsilon)$, of the respective cross sections in columns 2–4

| Energy (eV) | $\sigma_{diss,\,n,\,part}(\varepsilon)$ $CF_3$ | $\sigma_{diss,\,n,\,part}(\varepsilon)$ $CF_2$ | $\sigma_{diss,\,n,\,part}(\varepsilon)$ CF | $\sigma_{diss,\,n,\,t}(\varepsilon)$ |
|---|---|---|---|---|
| 20 | 0.006 | | 0.001 | 0.007 |
| 25 | 0.009 | | 0.012 | 0.021 |
| 30 | 0.014 | 0.0009 | 0.016 | 0.031 |
| 35 | 0.023 | 0.0016 | 0.017 | 0.042 |
| 40 | 0.030 | 0.0025 | 0.018 | 0.051 |
| 50 | 0.074 | 0.0047 | 0.017 | 0.096 |
| 60 | 0.101 | 0.0062 | 0.016 | 0.123 |
| 70 | 0.113 | 0.0066 | 0.015 | 0.135 |
| 80 | 0.116 | 0.0062 | 0.015 | 0.137 |
| 90 | 0.138 | 0.0058 | 0.015 | 0.159 |
| 100 | 0.149 | 0.0058 | 0.014 | 0.169 |
| 110 | 0.153 | 0.0059 | 0.016 | 0.175 |
| 120 | 0.145 | 0.0057 | 0.014 | 0.165 |
| 130 | 0.144 | 0.0054 | 0.014 | 0.163 |
| 140 | 0.137 | 0.0055 | 0.014 | 0.157 |
| 150 | 0.133 | 0.0050 | 0.012 | 0.150 |
| 160 | 0.137 | 0.0047 | 0.014 | 0.156 |
| 170 | 0.130 | 0.0046 | 0.015 | 0.150 |
| 180 | 0.133 | 0.0048 | 0.016 | 0.154 |
| 190 | 0.136 | 0.0046 | 0.012 | 0.153 |
| 200 | 0.135 | 0.0048 | 0.015 | 0.155 |

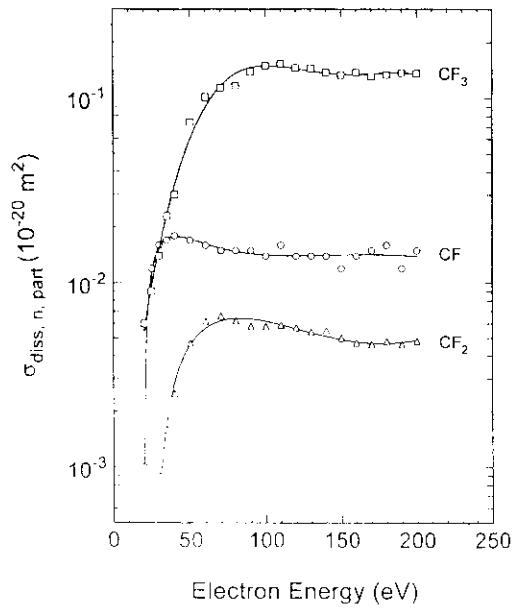


FIG. 10. Partial cross sections, $\sigma_{diss,\,n,\,part}(\varepsilon)$, for electron impact dissociation of $CHF_3$ into the neutral fragments $CF_3$, $CF_2$, and CF (data of Goto *et al.*—Ref. 29 as revised by Sugai *et al.*—Ref. 37).

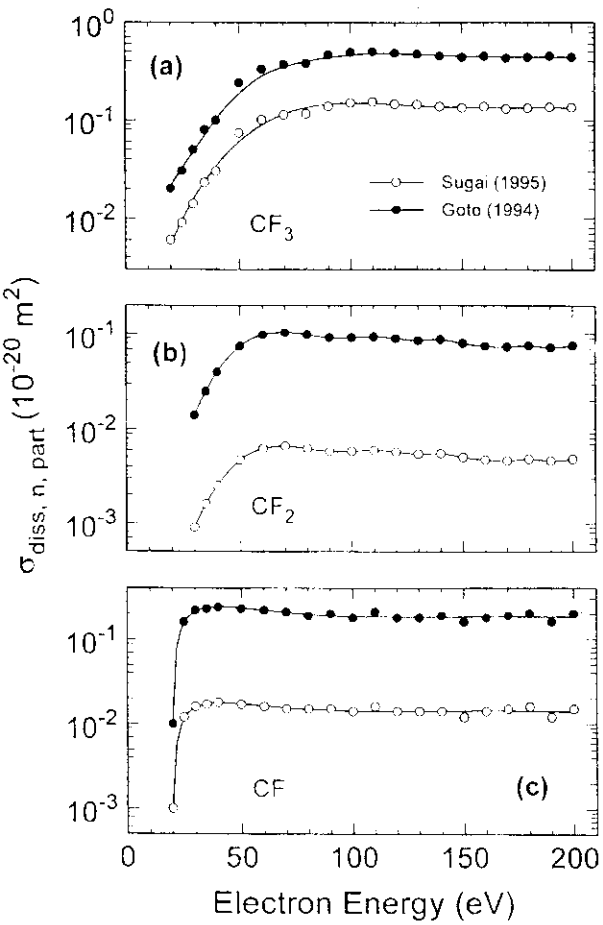


FIG. 11. Comparison of the original (Ref. 29) and the revised (Ref. 37) values of the partial cross sections, $\sigma_{diss,\,n,\,part}(\varepsilon)$, for electron impact dissociation of $CHF_3$ into the neutral fragments $CF_3$, $CF_2$, and CF.

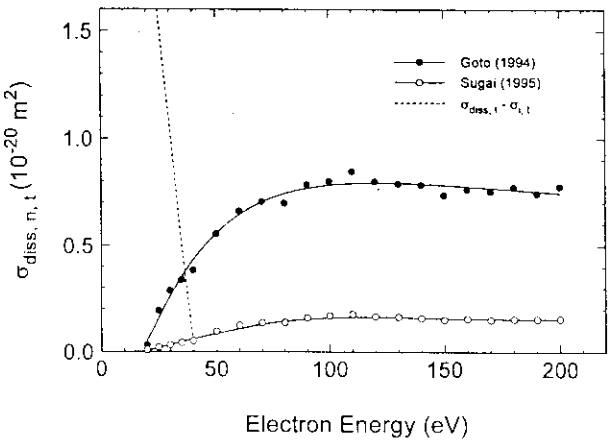


FIG. 12. Total cross section, $\sigma_{diss,\,n,\,t}(\varepsilon)$, for electron impact dissociation of $CHF_3$ into neutral species : ○, derived from the measurements of Goto *et al.*—Ref. 29 (column 7 of Table 11); ●, derived from the revised data of Sugai *et al.*—Ref. 37 (column 5 of Table 12). ---, $[\sigma_{diss,\,t}(\varepsilon) - \sigma_{i,\,t}(\varepsilon)]$ (see the text).

$\sigma_{diss,\,n,\,t}(\varepsilon)$ determined this way (dashed line in Fig. 12) clearly indicate that the data of Sugai *et al.*[37] may be grossly underestimating the magnitude of $\sigma_{diss,\,n,\,t}(\varepsilon)$. It might, of course, be possible that the values of Tarnovsky *et al.*[38,39] to which Sugai *et al.* normalized the Goto *et al.* data are themselves low. Clearly, more work is indicated.

Threshold energies for electron impact dissociation of $CHF_3$ into neutral species are listed in Table 13 as given by the authors. They help understand the energetics of the various dissociation processes leading to neutral fragments.

## 6. Electron Attachment

There have been a number of studies[40–50] on electron attachment to $CHF_3$, but the data are still fragmentary and no absolute cross sections as a function of electron energy have been reported for any of the negative ion fragments. The three mass spectrometric studies[40,43,49] are in agreement that the predominant dissociative electron attachment channels

TABLE 13. Threshold energies for electron impact dissociation of $CHF_3$ into neutral species[a] (from Goto *et al.*—Ref. 29—unless otherwise indicated)

| Reaction | Threshold energy (eV) |
|---|---|
| $CHF_3+e\rightarrow CF_3+H+e$ | 11.0[b,c] |
| $CHF_3+e\rightarrow CHF_2+F+e$ | 13.0[b,c] |
| $CHF_3+e\rightarrow CF_2+H+F+e$ | 15.0[b] |
| $CHF_3+e\rightarrow CF_2+HF+e$ | 9.1[b] |
| $CHF_3+e\rightarrow CHF+2F+e$ | 16.9[b] |
| $CHF_3+e\rightarrow CHF+F_2+e$ | 16.1 |
| $CHF_3+e\rightarrow CF+H+2F+e$ | 20.5[b] |
| $CHF_3+e\rightarrow CF+F_2+H+e$ | 19.7[b] |
| $CHF_3+e\rightarrow CF+HF+F+e$ | 14.6[b] |

[a]The $CF_3$–H bond dissociation energy is 4.46 ± 0.17 eV (Ref. 35).
[b]Expected value.
[c]Measured value; experimental uncertainty ±0.5 eV.

TABLE 14. Negative ion states of $CHF_3$

| Energy (eV) | Reference and method of observation |
|---|---|
| 2.9[a] | Dissociative electron attachment[b] |
| 3.7[a] | |
| 9.3[a] | |
| 0.04 | Electron swarm[c] |
| ~4.5(2.2±0.3)[d] | Dissociative electron attachment[e] |
| 10.1±0.1(8.2± 0.2)[d] | |
| 12.3±0.2(≤ 11)[d] | |
| 6.3(?)[f] | Electron transmission[g] |
| 9.3[f] | |
| 9.10[f] | Multiple scattering Xa (MS-$X_\alpha$) bound-state |
| 10.01[f] | calculations[g] |
| 9.44[f] | Continuum MS-Xa (CMS-$X_\alpha$) method[g] |
| 9.64[f] | |

[a]Thresholds of dissociative attachment processes.
[b]Reference 43.
[c]Data of Lee (Ref. 41) as analyzed by Blaunstein and Christophorou (Ref. 42).
[d]The first value is the energy position of the cross section maximum and the value in parentheses is the respective energy threshold.
[e]Reference 49.
[f]Vertical attachment energy.
[g]Reference 50.

are those leading to $F^-$. Actually, Reese *et al.*[40] and Scheunemann *et al.*[49] observed only $F^-$ while MacNeil and Thynne[43] reported the observation of $F^-$, $H^-$, $C^-$, $CH^-$, $CF^-$, $F_2^-$, $CF_2^-$, and $CF_3^-$, with the $F^-$ being by far the most abundant negative ion. Appearance onsets and peak energies for the $F^-$ negative ions from $CHF_3$ are given in Table 14. Table 14 also gives the vertical attachment energies measured in an electron transmission experiment[50] along with the vertical attachment energies obtained via bound and continuum multiple scattering $X_\alpha$ calculations.[50] Figure 13 shows[49] the yield for the formation of $F^-$ from $CHF_3$ as a function of electron energy. Clearly at least three

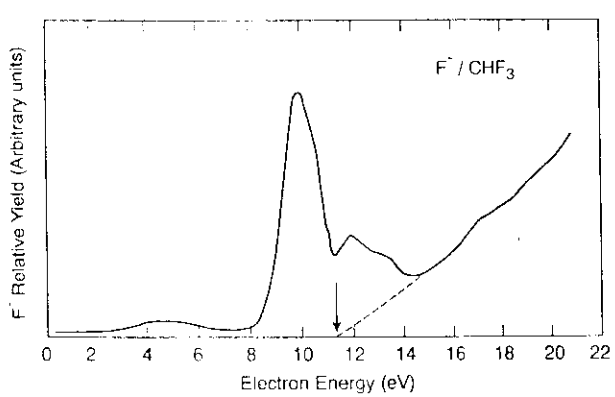


FIG. 13. Relative yield of $F^-$ produced by dissociative electron attachment to $CHF_3$. The rising part with an apparent onset at 11.5 eV (indicated by the arrow) is attributed to the nonresonant production of $F^-$ via the negative ion-positive ion pair process (from Scheunemann *et al.*—Ref. 29).

TABLE 15. Values of the thermal ($T \approx 295$ K) electron attachment rate constants, $(k_a)_{th}$, for $CHF_3$

| $(k_a)_{th}(10^{-14}$ cm$^3$ s$^{-1})$ | Reference |
|---|---|
| 4.6 | 44 |
| <6.2 | 45 |
| 3.6 | 46 |
| $1.1\times10^5$ | 41, 42 |

negative ion resonances lead to the production of $F^-$ below 14 eV. Depending on the energetics, a number of dissociative attachment processes,[43]

$$CHF_3 + e \rightarrow F^- + CHF_2 \quad (3a)$$

$$\rightarrow F^- + CHF + F \quad (3b)$$

$$\rightarrow F^- + CF_2 + H \quad (3c)$$

$$\rightarrow F^- + 2F + CH, \quad (3d)$$

can lead to the production of $F^-$. According to Scheunemann *et al.*,[49] the first resonance (~ 5 eV) is due to reaction (3a). The higher energy resonances at about 10 eV and 12 eV can be due to a multiplicity of fragmentation channels. It is interesting to note that the cross section for the production of $F^-$ via the 10 eV resonance far exceeds that from the lower lying resonance. The rise in the $F^-$ yield beyond about 14 eV has been attributed[49] to the positive ion-negative ion pair process

$$CHF_3 + e \rightarrow F^- + CHF_2^+ + e \quad (4)$$

for which Scheunemann *et al.*[49] have calculated a threshold of 11.5 eV±0.3 eV.

There have been a number of measurements of the thermal value of the rate constant, $(k_a)_{th}$, for electron attachment to $CHF_3$. These are listed in Table 15. With the exception of the earlier value based on the measurements of Lee,[41] all other values indicate that the rate constant for the attachment of thermal electrons to $CHF_3$ is very small. To our knowledge, no measurements of the density reduced electron attachment coefficient, $\eta/N$, or the density reduced electron impact ionization coefficient, $\alpha/N$, have been reported for $CHF_3$. They are being planned in our laboratory.

The most recent mass spectrometric measurements using a trochoidal monochromator as the electron source,[49] clearly show the existence of at least three negative-ion resonances leading to $F^-$ formation located at about 4.5 eV, 10.1 eV, and 12.3 eV (see Fig. 13). On the basis of these findings, it would be expected that the electron scattering cross sections (elastic and inelastic) from $CHF_3$ in this energy range will exhibit structure associated with these negative ion resonances. Additionally, by comparison to the electron attachment data on $CF_4$ (see Refs. 2 and 48) and methane,[47,48] the dissociative electron attachment to $CHF_3$ is expected to have a peak cross section value $>10^{-19}$ cm$^2$. Negative ions have been detected in rf plasmas of $CHF_3$ using a laser photodetachment method.[51] It is important to note that under high gas pressure conditions, a multitude of secondary negative

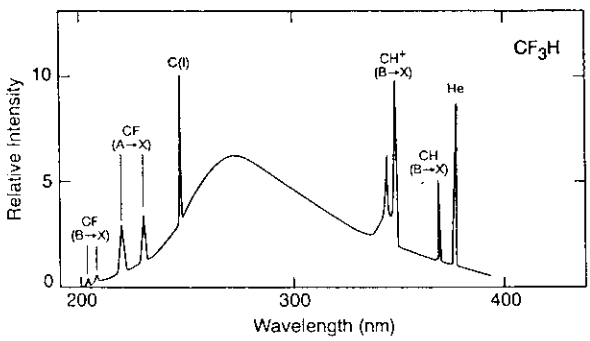


FIG. 14. Electron impact induced emission spectrum of $CHF_3$ in the wavelength range 200 nm to 400 nm (Ref. 57).

ions and negative ion clusters can form (see, e.g., Tiernan *et al.*[52]). For instance, the primary negative ion $F^-$ which is formed in the dissociative attachment of electrons to $CHF_3$ undergoes rapid ion-molecule reactions yielding[52] the cluster anions $(HF)_nF^-(n = 1-3)$.

## 7. Electron Transport

To our knowledge, no electron transport coefficient measurements have been made for $CHF_3$ except for a measurement of the ratio $w/(E/P)$ of the electron drift velocity, $w$, in $CHF_3$ over the pressure-reduced electric field, $E/P$, in the low $E/P$ region over which $w$ varies linearly with $E/P$. The value of this ratio at $T=295$ K was reported[25] to be $1.773 \times 10^7$ cm$^2$ Pa V$^{-1}$ s$^{-1}$ [ $= 13.3 \times 10^4$ cm$^2$ Torr V$^{-1}$ s$^{-1}$ (for $E/N < 3.69 \times 10^{-17}$ V cm$^2$)] and has been used to obtain an estimate of the electron scattering cross section at low energies (see Sec. 3 and Ref. 25).

The $CHF_3$ molecule is strongly polar[7,25] and has been used as the buffer gas in testing mixtures of weakly electron-attaching gases with strongly electron-attaching gases for gas dielectric purposes.[25,53–56] Mixtures of $CHF_3$ with electronegative gases that attach electrons over a wide range of electron energies above thermal[25,53] have been especially studied. The uniform field dielectric strength of $CHF_3$ has been reported[25] to be 0.27 that of $SF_6$, i.e., $\sim 97.5 \times 10^{-17}$ V cm$^2$. No measurements have been reported of the value, $(E/N)_{\text{lim}}$, of the density-reduced electric field, $E/N$, at which $\alpha/N = \eta/N$.

## 8. Electron Impact Induced Light Emission

A number of investigations have been made of light emission from $CHF_3$ under electron impact.[57–59] The first such study was by Van Sprang *et al.*[57] who used incident electron beam energies of 100 eV. The emission spectrum they obtained in the wavelength range 200 nm to 400 nm is reproduced in Fig. 14. Table 16 lists the emission cross sections measured by Van Sprang *et al.*[57] for the various atomic F and H lines for 100 eV incident electrons. Van Sprang *et al.*[57] also reported relative cross sections for the continuous emission from $CHF_3$ excited by electrons having kinetic

TABLE 16. Emission cross sections, $\sigma_{em}$ (100 eV), for various atomic F and H lines induced by impact of 100 eV electrons on $CHF_3$ (from Van Sprang *et al.*—Ref. 57)

| Emission line | Wavelength (nm) | $\sigma_{em}$ ($10^{-19}$ cm$^2$)[a] |
|---|---|---|
| F(I) $^2P_0 - ^2P$ | 703.7 | 1.5 |
| | 712.7 | 1.1 |
| F(I) $^2D_0 - ^2P$ | 760.7 | 0.7 |
| | 775.4 | 4.7 |
| | 780 | 1.9 |
| F(I) $^2S_0 - ^2P$ | 731.1 | 2.0 |
| F(I) $^4P_0 - ^4P$ | 733.1 | 1.8 |
| | 739.8 | 3.9 |
| | 742.5 | 1.1 |
| F(I) $^4D_0 - ^4P$ | 677.3 | 2.0 |
| | 685.6 | 5.9 |
| | 690.2 | 4.8 |
| $H_\alpha$ | 656.2 | 2.7 |
| $H_\beta$ | 486.1 | 5.7 |

[a]Quoted uncertainty ±10%.

energies from 20 eV to 2 000 eV. They ascribed the observed continua to the $C^2E - X^2A_1$ transition in $CHF_3^+$. (Continuous emission from $F_2$ also occurs[57] in the wavelength range 200 nm to 400 nm, because $F_2$ is a dissociation product of $CHF_3$.) In contrast with the Van Sprang *et al.* assignment of the continuous emission, Aarts[58] assigned the 230 nm to 350 nm emission band (the maximum intensity of this broad emission is around 270 nm) to the $CF_2$ $(\tilde{A} \rightarrow X)$ transition and this assignment was later confirmed by Creasy *et al.*[59] The threshold for the continuum emission was found[58] to be 14.1 eV±0.5 eV. Aarts used electrons with incident energies of up to 1 keV, and Creasy *et al.* used electron, photon, and metastable atom impact methods. Creasy *et al.* observed fluorescence which they associated with the $D^2A_1$ state of $CHF_3^+$ (adiabatic ionization energy 20.08 eV) (See also Lee *et al.*[60] concerning observation of fluorescence from $CHF_3^+$* under photoexcitation.) Aarts and Creasey reported emission spectra similar to those in Fig. 14. The emission cross section for the 270 nm band produced by electron impact on $CHF_3$ has been measured as a function of electron energy[58] and is listed in Table 17 and plotted in Fig. 15. Relative cross sections as a function of electron energy have also been reported by Van Sprang *et al.*[57]

Another important study dealing with light emission induced by electron impact on $CHF_3$ has been made by Wang and McConkey.[61] These investigators measured the emission spectrum of $CHF_3$ in the vacuum ultraviolet range (50 nm to 130 nm) under single collision conditions for incident electron energies up to 600 eV. The spectrum showed contributions from neutral and singly ionized fluorine and carbon fragments, and also from neutral hydrogen atoms. Wang and McConkey,[61] made absolute measurements of the cross sections for the F I and F II emissions in the range 75.1 nm to 97.77 nm, the C I and C II emissions in the range of 68.7 nm

TABLE 17. Cross section for the 270 nm continuous emission band produced by electron impact on $CHF_3$ (from Aarts—Ref. 58)

| Electron energy (eV) | Cross section ($10^{-18}$ cm$^2$)[a] |
|---|---|
| 14.1 | 0 |
| 30 | 5.4 |
| 40 | 5.8 |
| 45 | 6.1 |
| 50 | 5.8 |
| 60 | 5.4 |
| 80 | 5.2 |
| 100 | 4.8 |
| 150 | 4.6 |
| 200 | 4.5 |
| 300 | 3.4 |
| 400 | 3.2 |
| 500 | 2.7 |
| 600 | 2.4 |
| 800 | 2.0 |
| 1000 | 1.7 |

[a]The estimated reported uncertainty is about ±15%.

to 127.7 nm, and the hydrogen atom emissions in the range of 91.46 nm to 121.6 nm following impact of 200 eV incident electrons on $CHF_3$. The carbon emission cross sections are generally lower than the fluorine emission cross sections. The emission spectrum is dominated by the F I and H I emissions with the strongest lines at (78, 80.8, 95.5, 97.4 and 97.6) nm for F I, and the Ly $\alpha$ and Ly $\beta$ for H I. The cross sections at these wavelengths are $2.2\times10^{-19}$ cm$^2$, $3.3\times10^{-19}$ cm$^2$, $9.3\times10^{-19}$ cm$^2$, $5.9\times10^{-19}$ cm$^2$, $2.9\times10^{-19}$ cm$^2$, $27.1\times10^{-19}$ cm$^2$, and $6.5\times10^{-19}$ cm$^2$, respectively. All the major F I lines involve transitions of a $3s$ or $3d$ electron decaying to the ground state $1s^2 2s^2 2p^5\,^2P_{1/2,3/2}$ (for further details see Ref. 61).

Danilevskii *et al.*[62] also studied light emission from excited $CHF_3$ fragments formed by electron impact on $CHF_3$. They have reported measurements in the wavelength range of 300 nm to 850 nm for the effective excitation cross sections of excited F atoms, the Balmer series of the hydrogen atom, and the CH molecular fragment ($A^2\Delta \rightarrow X^2\Pi$) using 0.4 keV to 6 keV incident energy electrons. This incident electron energy is much larger than those used by Van Sprang *et al.*[57] and Wang and McConkey.[61] One, thus, would expect the cross sections of Danilevskii *et al.*[62] to be smaller. Their measured emission cross sections for 4 keV incident electrons are listed in Table 18. Interestingly, Danilevskii *et al.*[62] observed emission from only excited fragments.

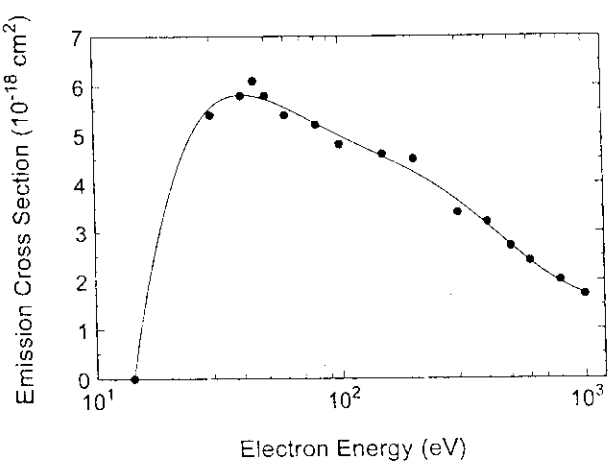


FIG. 15. Emission cross section for the 270 nm band in electron impact on $CHF_3$ as a function of incident electron energy (Ref. 58).

TABLE 18. Cross sections of emissions from excited F atoms, Balmer series lines of the hydrogen atom, and the CH molecular fragment ($A^2\Delta \rightarrow X^2\Pi$) formed by impact of 4 keV energy electrons on $CHF_3$ (from Ref. 62)

| Wavelength (nm) | Transition | Cross section ($10^{-21}$ cm$^2$) |
|---|---|---|
| F atom | | |
| 623.96 | $3s^4P-3p^4S^\circ$ | 14.2 |
| 634.85 | $3s^4P-3p^4S^\circ$ | 10.9 |
| 641.36 | $3s^4P-3p^4S^\circ$ | 10.0 |
| 669.05 | $3s^4P-3p^2D^\circ$ | 5.4 |
| 677.4 | $3s^4P-3p^4D^\circ$ | 7.0 |
| 683.4 | $3s^4P-3p^4D^\circ$ | 6.0 |
| 685.6 | $3s^4P-3p^4D^\circ$ | 17.3 |
| 687 | $3s^4P-3p^4D^\circ$ | 7.0 |
| 690.98 | $3s^4P-3p^4D^\circ$ | 10.2 |
| 733.2 | $3s^4P-3p^4P^\circ$ | 3.9 |
| 739.86 | $3s^4P-3p^4P^\circ$ | 8.5 |
| 703.75 | $3s^2P-3p^2P^\circ$ | 3.1 |
| 712.79 | $3s^2P-3d^2P^\circ$ | 2.6 |
| 720.26 | $3s^2P-3p^2P^\circ$ | 1.7 |
| 731.1 | $3s^2P-3p^2P^\circ$ | 4.9 |
| 775.47 | $3s^2P-3p^2D^\circ$ | 36.2 |
| CH($A^2\Delta-X^2\Pi$) | | 20.4 |
| $H_\alpha$ | | 184.6 |
| $H_\beta$ | | 19.4 |
| $H_\gamma$ | | 17.0 |
| $H_\delta$ | | 9.7 |

Their measured emission cross sections for 4 keV incident electrons are listed in Table 18. Interestingly, Danilevskii *et al.*[62] observed emission from only excited fragments.

The emission spectra of $CF_3$ radicals produced in the photolysis of $CHF_3$ have also been studied (see, e.g., Suto and coworkers[63]).

## 9. Electron Interactions with $CHF_3$ Fragments

Electron impact dissociation of the $CHF_3$ molecule produces $CF_3$, $CF_2$, and CF radicals which are common with radicals produced by electron impact on $CF_4$. For these three radicals cross sections for electron impact ionization producing the respective parent positive ions have been reported[38,39,64] and have been summarized and discussed in Ref. 2. Similarly, cross sections for electron impact dissociative ionization of these three radicals have been measured by Tarnovsky *et al.*[39] and have also been summarized in Ref. 2. No information exists on the other two possible fragments, $CHF_2$ and CHF, produced by electron impact on $CHF_3$.

Measurements of the concentrations of the $CF_3$, $CF_2$ and CF radicals in rf $CHF_3$ etching plasma have recently been made as a function of the microwave power and the gas

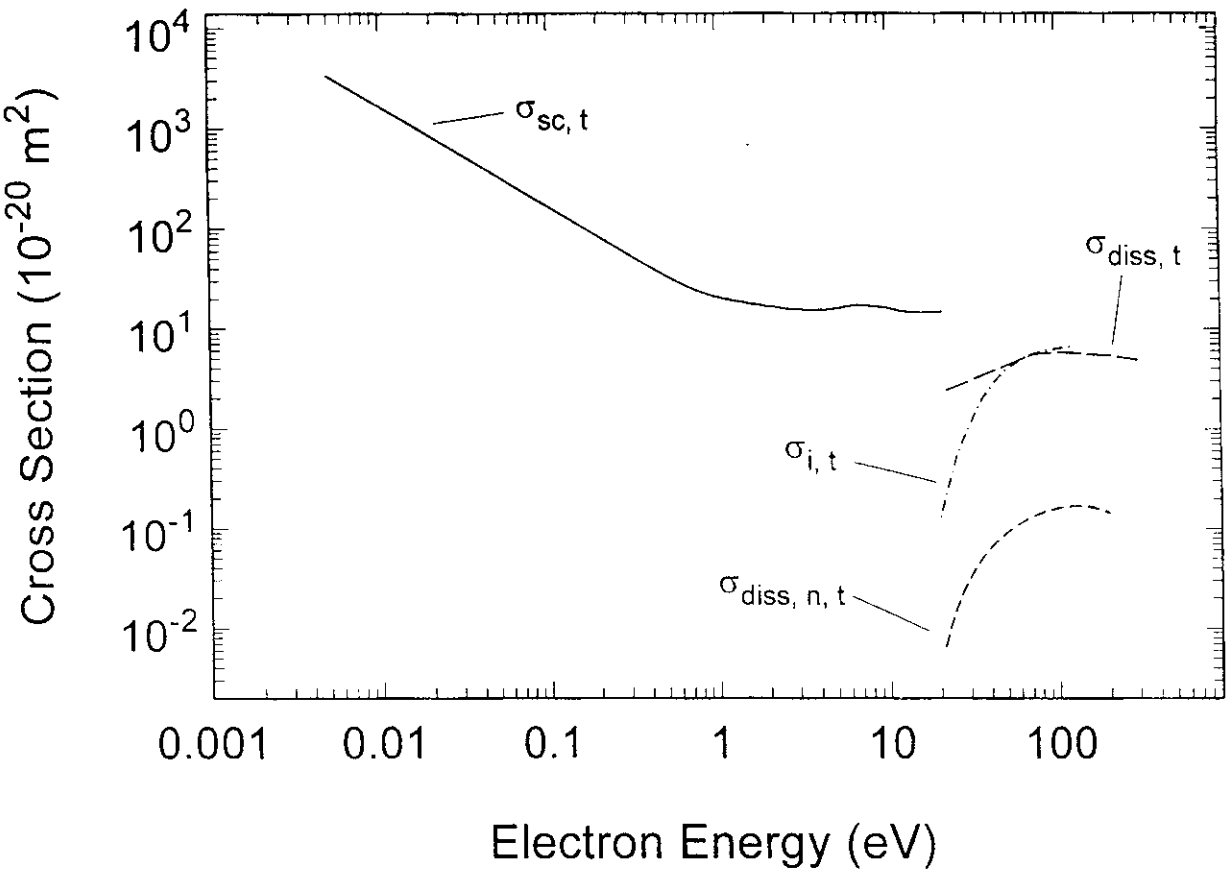


FIG. 16. Comparison of $\sigma_{sc,t}(\varepsilon)$, $\sigma_{i,t}(\varepsilon)$, $\sigma_{diss,t}$ and $\sigma_{diss,n,t}(\varepsilon)$.

pressure using infrared diode laser absorption spectroscopy.[65] The reader is referred to this source for details.

## 10. Summary of Cross Sections and Transport Coefficients

Unlike the case of $CF_4$ where sufficient data were available that allowed the recommendation[2] of cross sections for a number of electron collision processes, the limited amount of data for $CHF_3$ makes it difficult to recommend electron collision cross sections for this molecule. However, since such data may be currently needed to model plasma processing devices, we suggest the following cross sections:

(1) the total electron scattering cross section, $\sigma_{sc,t}(\varepsilon)$, in Table 5;
(2) the averaged total ionization cross section, $\sigma_{i,t}(\varepsilon)$, in Fig. 7 (solid line) (Table 8, column 5);
(3) the total dissociation cross section, $\sigma_{diss,t}(\varepsilon)$, in Fig. 8 (Table 10);
(4) the total cross section for dissociation into neutral fragments, $\sigma_{diss,n,t}(\varepsilon)$, in Fig. 12 (open triangles) (Table 12, column 5) of Sugai *et al.*[37] since it is the only direct measurement of this cross section (see Sec. 5 for a discussion of possible inconsistencies regarding the Sugai *et al.* data).

The cross sections just mentioned are plotted in Fig. 16; they are also available via the World Wide Web at http://www.eeel.nist.gov/811/refdata. They clearly show the limitations of the existing data and the large gap in the present database. Besides the recent unpublished measurements of Sanabia and Moore,[26] no cross sections of any kind exist in the important energy range between about 0.5 eV and 20 eV.

Data on electron transport coefficients for $CHF_3$ do not exist.

## 11. Needed Data

Basic measurements and calculations are needed for virtually all elastic and inelastic electron scattering processes, namely, cross sections for total, differential, and elastic electron scattering, cross section for momentum transfer, and cross sections for direct and indirect electronic, vibrational, and rotational excitation. Additional data are needed also for electron impact dissociation and ionization to resolve the apparent discrepancies between the direct measurement of $\sigma_{diss,n,t}(\varepsilon)$ and $\sigma_{i,t}(\varepsilon)$ and $\sigma_{diss,t}(\varepsilon)$. Measurements are necessary for all electron transport, attachment, and ionization coefficients over wide ranges of $E/N$.

## 12. Acknowledgments

We wish to thank J. Vergrugge for valuable assistance with the literature, Dr. R. J. Van Brunt and Dr. Y. Wang for

valuable comments, Dr. Y.-K. Kim for his unpublished data on the total ionization cross section, and Dr. J. Moore and J. Sanabia for their unpublished data on the total electron scattering cross section. This research has been sponsored in part by the U. S. Air Force Wright Laboratory under Contract No. F3361596-C-2600 with the University of Tennessee.

## 13. References

[1] The 1994 Report of the Scientific Assessment Working Group of IPCC, Intergovernmental Panel on Climate Change (unpublished), p. 28.
[2] L. G. Christophorou, J. K. Olthoff, and M. V. V. S. Rao, J. Phys. Chem. Ref. Data **25**, 1341 (1996).
[3] C. R. Brundle, M. B. Robin, and H. Basch, J. Chem. Phys. **53**, 2196 (1970).
[4] C. Y. R. Wu, L. C. Lee, and D. L. Judge, J. Chem. Phys. **71**, 5221 (1979).
[5] M. B. Robin, *Higher Excited States of Polyatomic Molecules* (Academic New York, 1974), Vol. I, pp. 178–191.
[6] J. F. Ying and K. T. Leung, Phys. Rev. A **53**, 1476 (1996).
[7] R. D. Nelson, Jr., D. R. Lide, Jr., and A. A. Maryott, *Selected Values of Electric Dipole Moments for Molecules in the Gas Phase*, NSRDS-NBS 10 (U.S. GPO, Washington, DC, 1967).
[8] W. L. Meerts and I. Ozier, J. Chem. Phys. **75**, 596 (1981).
[9] H. Sutter and R. H. Cole, J. Chem. Phys. **52**, 132 (1970).
[10] G. Cazzoli, L. Cludi, G. Cotti, L. Dore, C. D. Esposti, M. Bellini, and P. de Natale, J. Mol. Spectrosc. **163**, 521 (1994).
[11] J. A. Beran and L. Kevan, J. Phys. Chem. **73**, 3860 (1969).
[12] R. Kobayashi, R. D. Amos, H. Koch, and P. Jørgensen, Chem. Phys. Lett. **253**, 373 (1996).
[13] W. R. Harshbarger, M. B. Robin, and E. N. Lassettre, J. Electron Spectrosc. Relat. Phenom. **1**, 319 (1972/1973).
[14] C. Larrieu, M. Chaillet, and A. Dargelos, J. Chem. Phys. **94**, 1327 (1991).
[15] P. Sauvageau, R. Gilbert, P. P. Berlow, and C. Sandorfy, J. Chem. Phys. **59**, 762 (1973).
[16] S. Stokes and A. B. F. Duncan, J. Am. Chem. Soc. **80**, 6177 (1958).
[17] F. C.-Y. Wang and G. E. Leroi, Ann. Isr. Phys. Soc. **6**, 210 (1983).
[18] B. P. Pullen, T. A. Carlson, W. E. Moddeman, G. K. Schweitzer, W. E. Bull, and F. A. Grimm, J. Chem. Phys. **53**, 768 (1970).
[19] G. Bieri, L. Asbrink, and W. von Niessen, J. Electron Spectrosc. Relat. Phenom. **23**, 281 (1981).
[20] A. Campargue and F. Stoeckel, J. Chem. Phys. **85**, 1220 (1986).
[21] K. Kim and C. W. Park, J. Mol. Struct. **161**, 297 (1987); B. Galabov, T. Dudev, and W. J. Orville-Thomas, *ibid.* **145**, 1 (1986).
[22] S. Altshuler, Phys. Rev. **107**, 114 (1957).
[23] L. G. Christophorou and A. A. Christodoulides, J. Phys. B **2**, 71 (1969).
[24] L. G. Christophorou, *Atomic and Molecular Radiation Physics* (Wiley-Interscience, London, 1971), Chap. 4.
[25] L. G. Christophorou, D. R. James, and R. A. Mathis, J. Phys. D **14**, 675 (1981).
[26] J. Sanabia and J. Moore (private communication).
[27] J. A. LaVerne and A. Mozumder, Radiat. Res. **96**, 219 (1983).
[28] H. U. Poll and J. Meichsner, Contrib. Plasma Phys. **27**, 359 (1987).
[29] M. Goto, K. Nakamura, H. Toyoda, and H. Sugai, Jpn. J. Appl. Phys. **33**, 3602 (1994).
[30] J. A. Beran and L. Kevan, J. Phys. Chem. **73**, 3866 (1969).
[31] Y.-K. Kim (private communication).
[32] Y.-K. Kim and M. E. Rudd, Phys. Rev. A **50**, 3954 (1994); W. Hwang, Y.-K. Kim, and M. E. Rudd, J. Chem. Phys. **104**, 2956 (1996).
[33] H. F. Winters and M. Inokuti, Phys. Rev. A **25**, 1420 (1982).
[34] D. L. Hobrock and R. W. Kiser, J. Phys. Chem. **68**, 575 (1964).
[35] J. B. Farmer, I. H. S. Henderson, F. P. Lossing, and D. G. H. Marsden, J. Chem. Phys. **24**, 348 (1956).
[36] C. Lifshitz and F. A. Long, J. Phys. Chem. **69**, 3731 (1965).
[37] H. Sugai, H. Toyoda, T. Nakano, and M. Goto, Contrib. Plasma Phys. **35**, 415 (1995).
[38] V. Tarnovsky and K. Becker, J. Chem. Phys. **98**, 7868 (1993).
[39] V. Tarnovsky, P. Kurunczi, D. Rogozhnikov, and K. Becker, Int. J. Mass Spectrom. Ion Proc. **128**, 181 (1993).
[40] R. M. Reese, V. H. Dibeler, and F. L. Mohler, J. Res. Natl. Bur. Stand. **57**, 367 (1956).
[41] T. G. Lee, J. Phys. Chem. **67**, 360 (1963).
[42] R. P. Blaunstein and L. G. Christophorou, J. Chem. Phys. **49**, 1526 (1968).
[43] K. A. G. MacNeil and J. C. J. Thynne, Int. J. Mass Spectrom. Ion Phys. **2**, 1 (1969).
[44] R. W. Fessenden and K. M. Bansal, J. Chem. Phys. **53**, 3468 (1970).
[45] F. J. Davis, R. N. Compton, and D. R. Nelson, J. Chem. Phys. **59**, 2324 (1973).
[46] A. A. Christodoulides, R. Schumacher, and R. N. Schindler, Int. J. Chem. Kinet. **10**, 1215 (1978).
[47] L. G. Christophorou, D. L. McCorkle, and A. A. Christodoulides, in *Electron Molecule Interactions and Their Applications* (Academic, New York, 1984), Vol. 1, Chap. 6.
[48] L. G. Christophorou, Environ. Health Perspectives **36**, 3 (1980).
[49] H.-U. Scheunemann, M. Heni, E. Illenberger, and H. Baumgärtel, Ber. Bunsenges. Phys. Chem. **86**, 321 (1982).
[50] A. Modelli, F. Scagnolari, G. Distefano, D. Jones, and M. Guerra, J. Chem. Phys. **96**, 2061 (1992).
[51] M. Haverlag, A. Kono, D. Passchier, G. M. W. Kroesen, W. J. Goedheer, and F. J. de Hoog, J. Appl. Phys. **70**, 3472 (1991).
[52] T. O. Tiernan, C. Chang, and C. C. Cheng, Environ. Health Perspectives **36**, 47 (1980).
[53] L. G. Christophorou, D. R. James, and R. Y. Pai, in *Applied Atomic Collision Physics* (Academic, New York, 1982), Vol. 5, p. 87.
[54] L. G. Christophorou, D. R. James, I. Sauers, M. O. Pace, R. Y. Pai, and A. Fatheddin, in *Gaseous Dielectrics III* (Pergamon, New York, 1982), p. 151.
[55] EPRI Report No. EPRI EI-2620, September 1982.
[56] R. S. Nema, S. V. Kulkarni, and E. Husain, IEEE Trans. Electric. Insul. **EI-17**, 434 (1982).
[57] H. A. Van Sprang, H. H. Brongersma, and F. J. De Heer, Chem. Phys. **35**, 51 (1978).
[58] J. F. M. Aarts, Chem. Phys. **95**, 443 (1985).
[59] J. C. Creasey, I. R. Lambert, R. P. Tuckett, and A. Hopkirk, Mol. Phys. **71**, 1355 (1990).
[60] L. C. Lee, J. C. Han, C. Ye, and M. Suto, J. Chem. Phys. **92**, 133 (1990).
[61] S. Wang and J. W. McConkey, Can. J. Phys. **67**, 694 (1989).
[62] N. P. Danilevskii, I. Y. Rapp, V. T. Koppe, and A. G. Koval, Opt. Spectrosc. **60**, 441 (1986).
[63] M. Suto and N. Washida, J. Chem. Phys. **78**, 1007, 1012 (1983); M. Suto, N. Washida, H. Akimoto, and M. Nakamura, *ibid.* **78**, 1019 (1983); M. Suto and L. C. Lee, *ibid.* **79**, 1127 (1983).
[64] H. Deutsch, T. D. Märk, V. Tarnovsky, K. Becker, C. Cornelissen, L. Cespiva, and V. Bonacic-Koutecky, Int. J. Mass Spectrom. Ion Proc. **137**, 77 (1994).
[65] K. Takahashi, M. Hori, K. Maruyama, S. Kishimoto, and T. Goto, Jpn. J. Appl. Phys. **32**, L694 (1993); K. Takahashi, M. Hori, and T. Goto, *ibid.* **33**, 4745 (1994); K. Maruyama, K. Ohkouchi, Y. Ohtsu, and T. Goto, *ibid.* **33**, 4298 (1994); K. Takahashi, M. Hori, S. Kishimoto, and T. Goto, *ibid.* **33**, 4181 (1994).